

Coupling between phonons and intrinsic Josephson oscillations in cuprate superconductors

Ch. Helm, Ch. Preis, F. Forsthofer and J. Keller,
 Institut für Theoretische Physik, Universität Regensburg, D-93040 Regensburg, Germany
 K. Schlenga, R. Kleiner, and P. Müller,
 Physikalisches Institut III, Universität Erlangen-Nürnberg, D-91058 Erlangen, Germany
 (March 31, 2018, submitted to Physical Review Letters)

The recently reported subgap structures in the current-voltage characteristic of intrinsic Josephson junctions in the high- T_c superconductors $\text{Tl}_2\text{Ba}_2\text{Ca}_2\text{Cu}_3\text{O}_{10+\delta}$ and $\text{Bi}_2\text{Sr}_2\text{CaCu}_2\text{O}_{8+\delta}$ are explained by the coupling between c-axis phonons and Josephson oscillations. A model is developed where c-axis lattice vibrations between adjacent superconducting multilayers are excited by the Josephson oscillations in a resistive junction. The voltages of the lowest structures correspond well to the frequencies of longitudinal c-axis phonons with large oscillator strength in the two materials, providing a new measurement technique for this quantity.

The transport properties of highly anisotropic cuprate superconductors in c-direction can well be described by a stack of Josephson junctions formed by non-superconducting material between adjacent superconducting copper oxide multi-layers [1]. Recently the observation of subgap structures in the current-voltage (I - V)-characteristic of intrinsic Josephson junctions in the high- T_c superconductors $\text{Tl}_2\text{Ba}_2\text{Ca}_2\text{Cu}_3\text{O}_{10+\delta}$ (TBCCO) and $\text{Bi}_2\text{Sr}_2\text{CaCu}_2\text{O}_{8+\delta}$ (BSCCO) has been reported [2–4]. Each individual branch of the I - V -curve shows a structure which can be traced back to the I - V -characteristic of one single Josephson junction in the resistive state. These structures seem to be an intrinsic effect, as they have been observed both in step edge junctions (TBCCO) and mesa-type stacks (BSCCO) of different sizes. The characteristic voltages are completely independent of temperature and

external magnetic fields, which rules out any relation to the superconducting gap, vortex flow or the thermal excitation of quasiparticles.

It was shown that the pattern of one junction can be described phenomenologically by a resistively shunted junction (RSJ) model by assuming ad hoc a special structure for the current-voltage characteristic of the quasiparticles [3]. It was argued that such a structure might result from peaks in the quasiparticle density of states due to Andreev reflection between normal and superconducting regions. Several alternative approaches, including the modulation of the tunneling distance due to Raman-active phonons, have been mentioned in [2], but up to now all suggestions failed to explain the main features of the effect. In this paper we want to discuss a different mechanism involving phonons by assuming that the local electric field oscillations produced by the Josephson effect in a single junction excite infrared active c-axis phonons. In the following we will present a simple model where we couple the non-linear current-phase relation of one junction to a local oscillator. The analytical and numerical solution of this model provides a very good quantitative explanation of the experimental data. It is

shown that the peaks in the subgap structure of the dc current-voltage characteristic correspond to zeros of the dielectric function of the barrier material, i.e. to longitudinal optical phonons.

In the minimal version of the RSJ model the total current (density)

$$i = j_c \sin \gamma + \sigma_0 E + \dot{D}, \quad (1)$$

through one of the junctions is the sum of the Josephson current, the (ohmic) quasiparticle current $I_{\text{qp}} = \sigma_0 E$ and the displacement current density \dot{D} , where the (gauge invariant) phase difference γ is related to the electric field E in the barrier of thickness b by

$$\hbar\gamma = 2eEb. \quad (2)$$

Further time dependencies of a microscopic model are thereby neglected for simplicity [5,6].

The displacement current \dot{D} contains the polarization P of the barrier medium, $D = \epsilon_0 E + P = \epsilon_0 \epsilon E$. In the case of high frequency Josephson oscillations in the range of phonon frequencies it is important to keep the full frequency dependence of $\epsilon(\omega)$ or to treat the polarization P as an additional dynamical variable.

Here we assume that the polarization $P = nqz$ is due to a c-axis displacement z of ions with charge q , mass M and density n in the insulating barrier between the copper oxide (multi)-layers. For the motion of the ions we assume a simple oscillator

$$\ddot{z} + \omega_0^2 z + r\dot{z} = \frac{q}{M} E, \quad (3)$$

which is driven by the electric field E in the barrier. In this model the contribution of the oscillator to the dielectric function is given by

$$\epsilon_{\text{ph}}(\omega) = 1 + \frac{nq^2}{\epsilon_0 M} \frac{1}{\omega_0^2 - \omega^2 + ir\omega}. \quad (4)$$

It is useful to introduce normalized quantities: First equ. (1) and (3) are divided by the critical current density j_c , then a characteristic time variable $\tau = t\omega_c$ with $\omega_c = (2e/\hbar)V_c$ is introduced, where $V_c = RI_c = bj_c/\sigma_0$ is the characteristic voltage determined experimentally by the voltage on the resistive branch at the critical current. Then we obtain

$$j = \sin \gamma + \dot{\gamma} + \beta_c \ddot{\gamma} + \dot{p}, \quad (5)$$

$$\lambda \dot{\gamma} = \ddot{p} + \Omega^2 p + \rho \dot{p}, \quad (6)$$

with the normalized polarization $p = P\omega_c/j_c$, frequency $\Omega = \omega_0/\omega_c$, friction $\rho = r/\omega_c$ and the McCumber parameter $\beta_c = RC\omega_c = \omega_c^2/\omega_J^2$, where $\omega_J^2 = 2ebj_c/(\hbar\epsilon_0)$ is the square of the Josephson plasma frequency and $C = \epsilon_0 F/b$ is the capacitance of the barrier. The coupling constant $\lambda = \omega_{\text{ion}}^2/\omega_J^2 = S(\omega_0^2/\omega_J^2)$ can be expressed by the ionic plasma frequency $\omega_{\text{ion}}^2 = nq^2/(M\epsilon_0)$ or the oscillator strength S of the lattice vibration. In the present case the ratio between the phonon frequency ω_0 and the Josephson plasma frequency ω_J is large; therefore even a small oscillator strength $S = (\omega_{\text{ion}}^2/\omega_0^2)$ can lead to a sizable coupling.

The equations (5) and (6) for the phase and the lattice displacement can be solved numerically to yield $\gamma(t)$ as a function of the current density j through the junction. Taking a time average of the phase the dc current-voltage characteristic is obtained.

From the numerical results it turns out that both the phase $\gamma(t)$ and the polarization $p(t)$ oscillate primarily with one frequency, which is in agreement with general expectations for the RSJ-model with large β_c [6]. Therefore it is satisfied to neglect the higher harmonics in the ansatz

$$\gamma = \gamma_0 + vt + \gamma_1 \sin \omega t, \quad (7)$$

$$p = p_0 + p_1 \cos(\omega t + \varphi). \quad (8)$$

Here v is the time averaged phase velocity, which corresponds to the dc voltage $v = \langle V \rangle / V_c$ in the resistive state.

The different Fourier components of the equations of motion are obtained by the Bessel function expansion

$$\sin \gamma(t) = \sum_{n=-\infty}^{\infty} J_n(\gamma_1) \sin(\gamma_0 + vt + n\omega t). \quad (9)$$

The Josephson current contributes to the dc current only if $v + n\omega = 0$.

For the fundamental harmonic we obtain $\omega = v$. Using this ansatz in the differential equations (5) and (6) we obtain a set of equations for the amplitudes of the different Fourier components. As equ. (6) is linear in the polarization p , we can eliminate the polarization p and get an equation of motion for the phase oscillation alone:

$$j = v(1 + \frac{1}{2}\sigma(v)\gamma_1^2), \quad (10)$$

$$(J_0(\gamma_1) - J_2(\gamma_1)) \cos \gamma_0 = v^2 \beta_{\text{eff}}(v) \gamma_1, \quad (11)$$

$$J_1(\gamma_1) \sin \gamma_0 = -\frac{1}{2} v \sigma(v) \gamma_1^2 \quad (12)$$

with

$$\beta_{\text{eff}}(v) = \beta_c - \frac{\lambda(v^2 - \Omega^2)}{(v^2 - \Omega^2)^2 + v^2 \rho^2}, \quad (13)$$

$$\sigma(v) = 1 + \frac{\lambda v^2 \rho}{(v^2 - \Omega^2)^2 + v^2 \rho^2}. \quad (14)$$

The functions $\beta_{\text{eff}}(v)$ and $\sigma(v)$ are related to the real and imaginary part of the phonon dielectric function $\epsilon_{\text{ph}}(\omega) = \epsilon_1 + i\epsilon_2$ via

$$\beta_{\text{eff}}(v) = \beta_c \epsilon_1, \quad (15)$$

$$\sigma(v) = 1 + v\beta_c \epsilon_2. \quad (16)$$

Thereby the poles (zeros) of $\epsilon(\omega)$ are given by the eigenfrequencies ω_{TO} (ω_{LO}) of transversal (longitudinal) optical phonons for wavevectors $\vec{k} = 0$. In this way the formalism can be easily extended to an arbitrary number of phonon branches and more complicated lattice dynamical models.

As the numerical solution of equ. (5) and (6) shows that $\gamma_1 < 0.1$, the equations (10)-(12) can be linearized in γ_1 and an analytical formula for the I - V -characteristic can be obtained:

$$j(v) = v + \Delta j(v) = v + \frac{1}{2v} \frac{\sigma}{\sigma^2 + (v\beta_{\text{eff}})^2} \quad (17)$$

$$= v - \frac{1}{2v^2} \text{Im} \left(\frac{1}{\beta_{\text{eff}} + i\frac{\sigma}{v}} \right). \quad (18)$$

Higher orders in γ_1 have been calculated analytically, but have only a negligible influence on the I - V characteristic.

With the help of these relations some special points of the I - V -characteristic $j(v)$ near the subgap structures can be identified:

For small voltages $v \ll \Omega_{\text{TO}} = \Omega = \omega_{\text{TO}}/\omega_c$ one has $\beta_{\text{eff}}(v) \approx \beta_c$ and $\sigma(v) \approx 1$ and the model reduces to the conventional RSJ-model. For this it is well known [5] that there is a voltage jump in the I - V -characteristic at $v_{\text{min}} \approx 4\omega_J/(\pi\omega_c)$.

At the resonance $v = \Omega_{\text{TO}}$ of the phononic oscillator both the effective quasiparticle conductivity $\sigma(v)$ and the effective McCumber parameter β_{eff} are strongly enhanced and the I - V characteristic in equ. (18) reduces to the purely ohmic term. This corresponds to a pure quasiparticle tunneling current across the junction, while the supercurrent and the displacement current are compensating each other.

In contrast to this, equ. (18) indicates a resonance in $j(v)$ near the zeros of β_{eff} , i.e. the eigenfrequencies Ω_{LO} of *longitudinal* optical phonons.

The difference $\Delta v := \Omega_{\text{LO}} - v_{\text{max}}$ between Ω_{LO} and the actual maximum v_{max} of $j(v)$ can be estimated as $\Delta v < 2\%$, which is almost independent of the choice of

parameters. Physically this point is connected with an oscillation of the external electric field E and the polarization p with vanishing displacement current density \dot{D} . With the help of equ. (18) also an analytical formula for the intensity

$$\Delta j_{\max} := \Delta j(\Omega_{\text{LO}}) = \frac{1}{2\Omega_{\text{LO}}\sigma(\Omega_{\text{LO}})} \quad (19)$$

of the subgap structures can be derived. Thereby it turns out that a small damping parameter ρ , corresponding to a weak coupling of inter-layer ions in neighbouring contacts or equivalently the small dispersion of the phonons in c -direction, is crucial for the existence of a hysteretic region; no maximum of $j(v)$ can be found for $\rho \geq \rho_{\text{crit}} = \Omega_{\text{LO}} - \Omega_{\text{TO}}$. Also note that the intensity $\Delta i_{\max} = j_c \cdot \Delta j_{\max}$ in ordinary units is proportional to the critical current j_c , as it has been reported in experiments [3].

In addition to this, an analytical expression for the differential resistivity dv/dj can be derived, which is plotted in fig. 1. Note that there exists a region of negative differential resistivity for voltages v slightly larger than Ω_{LO} , which cannot be reached in a current-biased experiment with a continuously increasing (decreasing) bias current. The divergence of the differential resistivity at the subgap structures might be connected with experimental indications for a significantly enhanced noise production near the maxima of the I - V -characteristic.

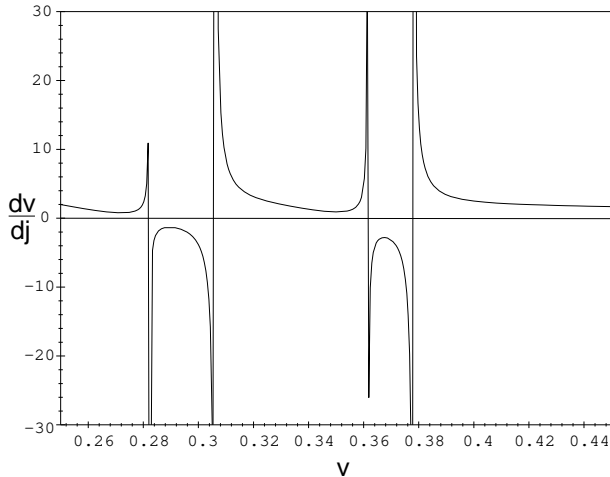


FIG. 1. Analytical solution for the differential resistivity for realistic TBCCO-parameters given in fig. 3.

The numerical solution of the differential equations (5) and (6) with a Runge-Kutta-algorithm is in excellent agreement with the analytical results given here, but it is difficult to investigate the region of the I - V -characteristic with negative differential resistivity with this method.

From general results for small capacity β_c [5] it is to be expected that the maximal current j_{\max} and the voltage v_{\max} of the peak is reduced in the presence of thermal noise. Consequently, the vanishing of the derivative $j'(v)$

near Ω_{LO} is rarely observed in experiments or numerical calculations.

In order to reproduce the experimental data in full detail, the shape of the quasiparticle characteristic I_{qp} has to be modified. Instead of the ohmic term $I_{\text{qp}} = \sigma_0 \dot{\gamma}$ in equ. (1) an exponential behaviour

$$I_{\text{qp}}(\dot{\gamma}) = \exp\left(\frac{\dot{\gamma} - 1}{v_b}\right) \quad (20)$$

for BSCCO and a semiconductor-like dependence

$$I_{\text{qp}}(\dot{\gamma}) = \frac{2\dot{\gamma}}{1 + \exp\left(\frac{1-\dot{\gamma}}{v_b}\right)} \quad (21)$$

for TBCCO have been used with an appropriate value of v_b successfully. The main consequence is a non-linear background $I_{\text{qp}}(v)$ in the I - V -characteristic, while the modifications of the quasiparticle conductivity $\sigma(v)$ are negligible. The shape and the position of the subgap structures are almost independent of the choice of $I_{\text{qp}}(\dot{\gamma})$ and the parameter v_b can be determined very well from parts of the I - V -characteristic away from the subgap structures.

For an appropriate choice of parameters these analytical and numerical results are in excellent agreement with the experimental data, as can be seen in figures (2) and (3). All experimental investigations of phonons in TBCCO [7] and BSCCO [8] agree that infrared active c -axis phonons are observed in the frequency range of the subgap structures. Theoretical calculations [9] show that the dispersion in c -direction is small, which corresponds to a small ratio $\rho/(\Omega_{\text{LO}} - \Omega_{\text{TO}})$ in our model. But considerable discrepancies in the published phonon data do not allow us to use the values given in the literature directly as input parameters. This is also due to the fact that usually only transversal frequencies are determined in optical experiments or model calculations, while the subgap structures should rather be compared with longitudinal branches. Also the precise values of the McCumber parameter β_c and the coupling constant λ in TBCCO and BSCCO are unknown. Therefore the experimental I - V -characteristics have been fitted with the unconstrained parameters $\beta_c, \Omega_i, \lambda_i, \rho_i$, which turns out to be quite a sensitive method for the determination of these quantities, as an optimal fit seems to be possible only in a very restricted parameter range. As shown above the position of the peaks is given by the zeros of the phonon dielectric constant, which is only dependent on the TO-frequencies Ω_i and the ratios λ_i/β . The absolute values of λ_i and β_c can be used to tune the relative strength of the peaks, while the values of ρ_i are important for the overall curvature of the structure.

The best fits for TBCCO and BSCCO are given in figures (2) and (3). The prediction for the eigenfrequencies $\nu_{\text{LO}} = \omega_{\text{LO}}(k=0)/(2\pi)$ of the longitudinal optical phonons with lowest frequencies in both materials are in ordinary units: $\nu_{\text{LO},1}=3.65$ THz and $\nu_{\text{LO},2}=4.70$ THz for

TBCCO with a characteristic voltage $V_c = 27.1\text{mV}$ and $\nu_{\text{LO},1}=2.96\text{ THz}$, $\nu_{\text{LO},2}=3.90\text{ THz}$ and $\nu_{\text{LO},3}=5.71\text{ THz}$ for BSCCO with $V_c = 21.8\text{mV}$. These values are compatible with the results of most optical experiments [7,8].

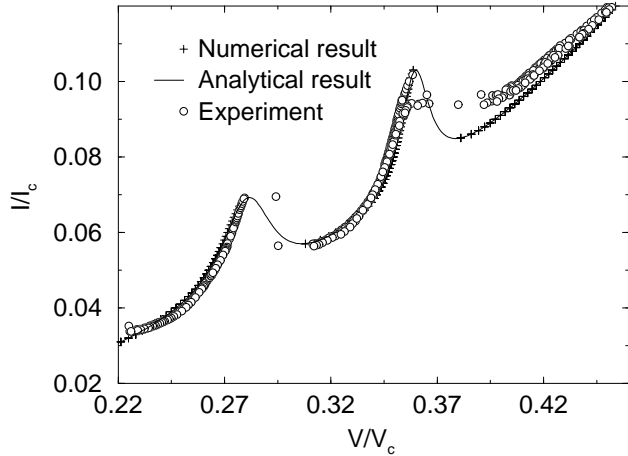


FIG. 2. Experimental, analytical and numerical I - V -characteristic of TBCCO for $\beta_c = 375$, $v_b = 0.29$, $\Omega_1 = 0.25$, $\lambda_1 = 8$, $\rho_1 = 0.03$, $\Omega_2 = 0.34$, $\lambda_2 = 3.5$, $\rho_2 = 0.015$.

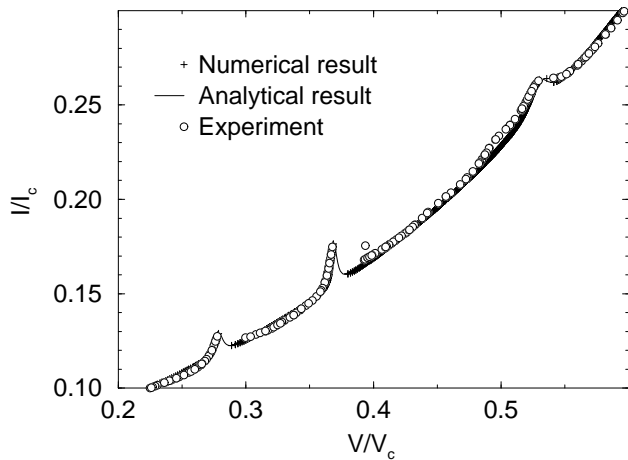


FIG. 3. Experimental, analytical and numerical I - V -characteristic of BSCCO for $\beta_c = 800$, $v_b = 0.337$, $\Omega_1 = 0.267$, $\lambda_1 = 10$, $\rho_1 = 0.008$, $\Omega_2 = 0.345$, $\lambda_2 = 19$, $\rho_2 = 0.0045$, $\Omega_3 = 0.468$, $\lambda_3 = 39$, $\rho_3 = 0.02$.

To summarize, the recently discovered subgap structures in the I - V -characteristic in the intrinsic Josephson effect in high- T_c -superconductors are explained by a coupling of Josephson oscillations to optical c -axis phonons within a modified RSJ-model. This is – to the knowledge of the authors – the first time that a detailed theoretical explanation of this effect has been given. Apart from perfect reproduction of the experimental data for both BSCCO and TBCCO new insights in the physical interpretation of the peak structures are obtained. Above all, the peak position is identified with the eigenfrequency of the longitudinal optical phonon, which provides a natural explanation for the crucial, experimental

result of the complete independence of the peak position on temperature, magnetic field and the geometry of the probe. In contrast to this, the position of the subgap structures is expected to depend on pressure and the isotopes contained in the material. This fact also suggests a new approach for a direct measurement of this quantity, which is usually hard to determine in optical experiments. It also turned out that the width of the structure is closely connected with the LO-TO-splitting of the phonon branch. Also the observed proportionality of the intensity of the resonance to the critical current can be understood within the model presented above.

In principle, similar structures in the current-voltage characteristic can be expected near the zeros of the corresponding dielectric constant, if other kinds of excitations with a dipole moment are coupled to Josephson oscillations between the layers in a similar way. Extensions of this work to a microscopic theory of the Josephson effect within the tunneling Hamiltonian formalism in the presence of phonon bands $\Omega(k_z)$ are currently being investigated. This might help to clarify the reason for the stability of a *local* oscillation despite of the finite coupling of oscillating ions in neighbouring junctions.

Acknowledgment: This work has been supported by a grant of the Bayerische Forschungsförderung within the research program FORSUPRA and by the Studienstiftung des Deutschen Volkes (C.H.).

-
- [1] R. Kleiner, F. Steinmeyer, G. Kunkel, and P. Müller, Phys. Rev. Lett. 68, 2394 (1992); R. Kleiner, and P. Müller, Phys. Rev. B 49, 1327 (1994).
 - [2] A. Yurgens, D. Winkler, N. Zavaritsky, and T. Claeson, SPIE Proceedings, Conference on Oxide Superconductor Physics and Nano-Engineering II, vol. 2697 (1996).
 - [3] K. Schlenga, G. Hechtfischer, R. Kleiner, W. Walkenhorst, P. Müller, H.L. Johnson, M. Veith, W. Brodkorb, and E. Steinbeiß, Phys. Rev. Lett. 76, 4993 (1996).
 - [4] P. Seidel, A. Pfuch, U. Hübner, F. Schmidl, H. Schneidewind, T. Ecke, J. Scherbel, submitted to Physica C.
 - [5] A. Barone, and G. Paterno. "Physics and Application of the Josephson effect". Wiley, New York, 1982.
 - [6] Konstantin K. Likharev "Dynamics of Josephson Junctions and Circuits". Gordon and Breach, 1996.
 - [7] T. Zetterer, M. Franz, J. Schützmann, W. Ose, H.H. Otto, and K.F. Renk, Phys. Rev. B 41, 9499 (1990); V.M. Burlakov, S.V. Shulga, J. Keller, and K.F. Renk, Physica C, 203, 68 (1992) and references therein.
 - [8] R. G. Buckley, M.P. Staines, D.M. Pooke, T. Stoto, and N.E. Flower, Physica C 248, 247 (1995) and references therein.
 - [9] J. Prade, A.D. Kulkarni, F.W. de Wette, U. Schröder, and W. Kress, Phys. Rev. B 39, 2771 (1989); A. D. Kulkarni, F.W. de Wette, J. Prade, U. Schröder, and W. Kress, Phys. Rev. B 43, 7, 5451 (1991).